Check for updates

*CORRESPONDENCE
Zishu Pan
zspan@whu.edu.cn

†PRESENT ADDRESS
Lei Lei,
Department of Microbiology and
Immunology, The University of Iowa,
Iowa City, IA, United States

Virus-like particles containing a prefusion-stabilized F protein induce a balanced immune response and confer protection against respiratory syncytial virus infection in mice

Jin Luo, Huan Qin, Lei Lei†, Wange Lou, Ruitong Li
and Zishu Pan ID*

State Key Laboratory of Virology, College of Life Sciences, Wuhan University, Wuhan, China

Respiratory syncytial virus (RSV) is a serious respiratory pathogen in infants and young children worldwide. Currently, no licensed RSV vaccines are available. In this study, we explored stable prefusion conformation virus-like particles (Pre-F VLPs) as RSV vaccine candidates. RSV fusion (F) protein mutants were constructed to form stabilized Pre-F or postfusion (Post-F) configurations. VLPs containing Pre-F or Post-F protein were generated using a recombinant baculovirus (rBV)-insect cell expression system. The assembly and immunological properties of Pre-F or Post-F VLPs were investigated. Pre-F and Post-F VLPs contained antigenic sites Ø and I of pre- and postfusion conformations, respectively. Compared with Post-F VLPs, immunization with Pre-F VLPs elicited upregulation of IFN-γ, IL-2 and IL-10 and downregulation of IL-4 and IL-5 cytokine production in mice. A high percentage of CD25$^+$ Foxp3$^+$ cells or a low percentage of IL-17A-producing cells among CD4$^+$ T cells was observed in the lungs of mice vaccinated with Pre-F VLPs. Importantly, immunization with Pre-F VLPs induced a high level of RSV neutralizing antibody and a balanced immune response, which protected mice against RSV infection without evidence of immunopathology. Our results suggested that Pre-F VLPs generated from rBV-insect cells represent promising RSV vaccine candidates.

KEYWORDS

respiratory syncytial virus, virus-like particles, vaccine, prefusion F protein, postfusion F protein, baculovirus insect cell expression system

Introduction

Human respiratory syncytial virus (RSV) was ascertained as a leading cause of bronchiolitis in infants as early as 1956 (1, 2). RSV infection causes a substantial disease burden in infant, immunocompromised, and elderly populations (3–5). Natural RSV infection does not induce sustained immunity, and repeated infections occur throughout life (6, 7). Therefore, it is particularly urgent to develop effective treatments and vaccines for RSV infection. Despite extensive efforts, no licensed RSV vaccines are available. Vaccination with formalin-inactivated RSV (FI-RSV) in the 1960s led to vaccine-enhanced disease (VED) upon RSV challenge (8–10), thus impeding RSV vaccine development. Intensive investigation showed that VED exhibited a strong relationship with the exaggerated Th2-type immune response and the poorly neutralizing antibodies upon RSV infection (11–14). Therefore, induction of a Th1-biased, balanced immune response and high neutralizing antibody production are critical for an effective RSV vaccine (15).

The RSV fusion (F) and attachment (G) glycoproteins presented on the virions are the major targets for RSV vaccine candidates (16–19). The F glycoprotein, which induces high neutralizing antibody titres and specific cellular immunity, provides immune protection and cross-protection against different RSV strains (20, 21). Crystal structures of both prefusion (Pre-F) and postfusion (Post-F) forms provided structural insights into the antigenicity of RSV F protein (22, 23), demonstrating that vaccines based on the Pre-F configuration represent promising next-generation vaccine candidates (24–26). A Pre-F form of the F protein contains an antigenic site Ø, which is not present in its Post-F conformation (27). Specific monoclonal antibodies directed to site Ø exhibited good RSV neutralizing ability (22). The engineered Pre-F protein exhibited enhanced physical and antigenic stability relative to DS-Cav1 (28, 29). A stabilized Pre-F protein elicited significantly increased neutralizing antibody titres compared with the Post-F form in animals, suggesting that a stable Pre-F protein represents a promising strategy for RSV vaccine candidate (27, 30–32).

Virus-like particles (VLPs) are effective, safe and promising vaccine platforms (33, 34). VLPs are genetically engineered complexes of multiple copies of protein antigens in a virus-like structure; VLPs lack viral genetic material and therefore cannot replicate (35, 36). Commercial VLP-based licensed vaccines are available against human papilloma and hepatitis B viruses (36). RSV glycoproteins presented as VLPs are highly immunogenic and confer protection against RSV infection (37–40). In the present study, we produced and characterized VLPs containing the stable prefusion and postfusion forms of the RSV F protein using an rBV-insect cell expression system. Immune responses and protection against RSV challenge induced by these VLPs were investigated in BALB/c mice.

Materials and methods

Cells, viruses, and preparation of ultraviolet (UV)-inactivated virus and antibodies

HEp-2 and Vero cells were obtained from the China Center for Type Culture Collection (CCTCC; Wuhan, China) and grown in Dulbecco's modified Eagle's medium (DMEM) supplemented with 10% foetal bovine serum (FBS, Gibco), 100 IU of penicillin, and 100 mg/ml streptomycin at 37°C and 5% CO_2. The respiratory syncytial virus (RSV) A2 strain was maintained in our laboratory. *Spodoptera frugiperda* 9 (Sf9) cells were obtained from the American Type Culture Collection (ATCC, Rockville, MD, USA) and cultured at 27°C in SF-900 II serum-free medium (SFM) (Invitrogen, USA), 100 IU penicillin and 100 mg/ml streptomycin. RSV was propagated in HEp-2 cells, and virus titres were quantified in Vero cells. RSV purification and inactivation by UV light was performed as previously described (18, 39). Briefly, RSV-infected HEp-2 cells were sonicated, clarified by centrifugation (1,200 × g for 30 min at 4°C) and concentrated by ultracentrifugation (120,000 ×g at 4°C for 6 h). The resultant precipitate was resuspended in phosphate-buffered saline (PBS) for RSV titration. For RSV purification, the resultant precipitate was resuspended in 10% sucrose in PBS; layered on top of a discontinuous sucrose gradient composed of 2 ml of 60%, 45%, and 30% sucrose (in PBS); and then centrifuged at 160,000 × g in a SW28 rotor for 2 h. The visible virus band between the 30% and 45% sucrose layers was collected for subsequent assays. For virus inactivation, 0.5 ml of a purified RSV suspension (10^6 PFU/ml) in a 35-mm petri dish was irradiated with ultraviolet (UV) light for 40 min, and the efficacy of UV inactivation was examined by determining the infectivity of inactivated RSV in Vero cells using a plaque assay. Mouse anti-F monoclonal antibody (mAb) clone 131-2A (Millipore, Temecula, USA), human anti-F mAb clone D25 (Cambridge Biologics, Boston, USA), goat anti-mouse IgG coupled to horseradish peroxidase (HRP) (Abclonal, Wuhan, China), and goat anti-human IgG coupled to HRP (Abclonal) were used in VLP binding assays.

Construction of plasmids and recombinant baculoviruses

The Pre-F and Post-F forms of RSV F protein (GenBank: ACO83301.1) were prepared as previously described (29, 41, 42). To obtain the stable prefusion F conformation protein, the site mutations N67I, S215P, and D486N were introduced into the F fragment. Then, the sequence encoding the T4 fibritin trimerization domain (foldon, SAIGGYIPEAPRDGQAYVRKDGEWVLLSTFL) was inserted into the position at amino acids 513 to 514 of the F

sequence. Subsequently, the P27 (amino acids 110-136) of the F protein was substituted with the linker (GSGSGRS) to generate a prefusion-stabilized F construct with the transmembrane (TM) and cytoplasmic domains (CT) in the $F_{514-574}$ location (Figure 1A). Similarly, the stable postfusion F form was constructed by deleting the sequence encoding amino acids 137 to 146 of the F protein. The sequence encoding the Pre-F, Post-F conformation, or IAV M1 gene (GenBank: ACP44152.1) was codon optimized for insect codon usage and synthesized by Sangon Biotech (Shanghai, China).

The Pre-F fragment was PCR-amplified using primers Pre-F/F and Pre-F/R with the *EcoR* I and *Xbal* I enzyme sites. The amplified product was digested with *EcoR* I and *Xbal* I and cloned into the *EcoR* I/*Xbal* I-digested pFBDM vector under the control of the promoter polyhedrin (pH) to generate the plasmid pFBDM-Pre-F. Similarly, the Post-F fragment or IAV M1 gene was amplified using primers Post-F-F/R or M1-F/R with the *EcoR* I and *Xbal* I enzyme sites and cloned into the pFBDM to generate the plasmid pFBDM-Post-F or pFBDM-M1, respectively. All specific primers used are listed in Table 1.

The identities of the plasmid constructs were verified by sequencing and subsequently used to generate recombinant baculovirus rBV-RSV-Pre-F, rBV-RSV-Post-F, or rBV-IAV-M1, as previously described (17, 43). In brief, the plasmids pFBDM-Pre-F, pFBDM-Post-F, and pFBDM-M1 were transformed into competent *E. coli* DH10 MultiBac cells to generate recombinant bacmids. The resultant bacmid DNA was separately transfected into Sf9 insect cells to obtain the corresponding recombinant baculovirus designated rBV-RSV-Pre-F, rBV-RSV-Post-F, or rBV-IAV-M1.

Production and purification of chimeric VLPs

The RSV Pre-F VLPs and Post-F VLPs were produced by Sf9 cells coinfected with rBV-RSV-Pre-F and rBV-IAV-M1 or rBV-RSV-Post-F and rBV-IAV-M1 (MOI=1 for each rBV). rBV-infected Sf9 cells were cultured in SF-900 II SFM at 27°C for 3 days. Then, the cultured Sf9 cells were collected by

centrifugation and lysed and frozen once at -80°C, and the cell lysates were clarified at 5000 rpm for 30 min. The VLP-containing supernatant was centrifuged at 60000×g and 4°C for 4 h, and the pellets were collected and resuspended in phosphate buffer (0.15 M NaCl, 0.05 M phosphate, pH 7.2). The protein samples were purified using HiPrep Sephacryl S-500 HR (GE Healthcare, Freiburg, Germany) in phosphate buffer at a flow rate of 0.5 ml/min as recommended by the manufacturer. Purified VLPs were quantified using the Bradford protein assay kit (Sangon Co., Ltd.) according to the manufacturer's instructions.

SDS–PAGE, Western blot analysis and electron microscopy observation

The expressed proteins were characterized by SDS–PAGE, western blotting and electron microscope observation as previously described (44). In brief, the prepared samples were separated on 12% polyacrylamide gels and stained with Coomassie blue R250 or transferred onto PVDF membranes for western blot analysis using a mouse anti-F mAb clone 131-2A (Millipore) or a mouse anti-M1 mAb clone 36H4 (Immune Tech, New York, USA). The purified RSV Pre-F or Post-F VLPs adsorbed onto copper grids were negatively stained with 2% phosphotungstic acid and observed with a transmission electron microscope (JEM-2100, JEOL, Tokyo, Japan).

Immunization and challenge of mice

Specific-pathogen-free (SPF) female BALB/c mice (Wuhan University Center for Animal Experiments) aged 6-8 weeks old were intramuscularly (i.m.) immunized thrice at 2-week intervals with 10 µg VLPs in 100 µl (45, 46). For the UV-RSV control, mice were immunized i.m. with 1×10^5 PFU of purified UV-RSV in 100 µl (18). For the PBS control, mice were inoculated i.m. with 100 µl PBS. Blood was collected by tail vein puncture during preimmunization and at 2 weeks after the

FIGURE 1
Construction of recombinant baculoviruses and expression of proteins in Sf9. **(A)** Schematic representation of the recombinant baculovirus vectors used in the present study. pH, polyhedrin promoter of baculovirus; **(B)** Coexpression of the RSV F and H1N1 M1 proteins in Sf9 cells. Sf9 cells were infected with the indicated rBVs, harvested at 3 days postinfection (p.i.) and subjected to Western blot analysis using a mouse monoclonal anti-RSV F antibody and a mouse polyclonal anti-H1N1 M1 antibody. M, Molecular marker; Lane 1, rBV-RSV-Pre-F/M1; Lane 2, rBV-RSV-Post-F/M1; Lane 3, Sf9 cells.
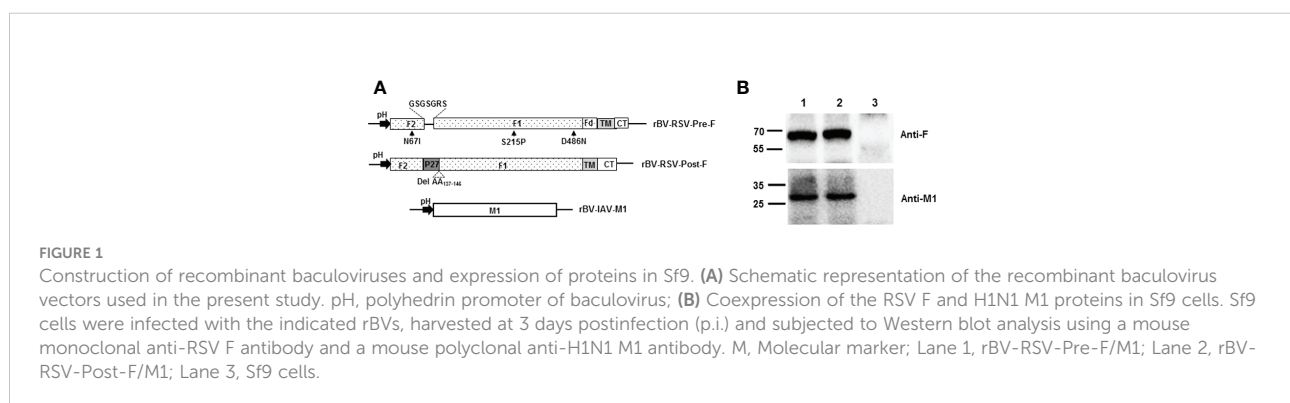
TABLE 1 Oligonucleotides in specific primers for the construction of recombinant plasmids.

Primer	Nucleotide sequence (5′ - 3′)	Enzyme
PreF-F	CGGAATTC**GCCACC**ATGGAACTGCTGA	EcoR I
PreF-R	GCTCTAGATTAGTTTGAGAAAGCGATGTTGTTGATTCC	Xbal I
PostF-F	CGGAATTC**GCCACC**ATGGAGTTGCTA	EcoR I
PostF-R	GCTCTAGATTAGTTACTAAATGCAATATTATTTATACCAC	Xbal I
M1-F	CGGAATTC**GCCACC**ATGAGCCTGCTGACCGAGGTGGAGACCTAC	EcoR I
M1-R	GCTCTAGATCACTTGAAACGCTGCATCTGCAC	Xbal I
RSV N-F	GGTGGAGAAGCAGGATTCTACCATATATTG	For qRT–PCR
RSV N-R	CTGTATTCTCCCATTATGCCTAGGCC	

Underlined sequences represent restriction enzyme sites. Bolded regions indicate Kozak coding sequences.

final immunization for antibody detection, and splenocytes were isolated for cytokine detection.

For histological analysis, mice were intranasally (i.n.) challenged with 3×10^6 PFU of RSV A2 in 100 µl at 2 weeks after the final immunization. The whole lungs of three mice were harvested on Day 4 following RSV challenge, immersed in 4% paraformaldehyde, embedded in paraffin and sectioned. The tissue sections were stained with haematoxylin and eosin (H&E) for routine evaluation and with periodic acid-Schiff (PAS) staining of amylase-treated tissue for observation of mucus secretion. The lung inflammation scores were defined as previously described (16, 44), where 0 indicates no inflammation, 1 indicates minimal inflammation, 2 indicates mild inflammation, 3 indicates moderate inflammation, and 4 indicates marked inflammation. Mucus hypersecretion scores in airways were defined as follows: 1-no mucus detectable, 2-rare mucus, 3-moderate mucus accumulation, 4-severe mucus production (47).

ELISA

Virus-specific IgG, IgG2a, and IgG1 antibodies in mouse sera were determined by enzyme-linked immunosorbent assay (ELISA) using RSV as the coating antigen (18, 48). Briefly, each well of a 96-well plate was coated with 100 µl of purified inactivated RSV (1×10^5 PFU/well). Serial dilutions of mouse sera in PBS/Tween-20 (PBS-T) containing 1% BSA were added to the wells and incubated at 37°C for 1 h. An HRP-conjugated goat anti-mouse IgG, IgG2a, or IgG1 mAb (Abclonal) was used as the secondary antibody.

Cytokine concentrations in the splenocytes or lung homogenates were quantified by ELISA as previously described (17). Regarding splenocyte cytokines, splenocyte suspensions were prepared from the spleens of experimental mice using Mouse 1×Lymphocyte Separation Medium (Dakewe Biotech, Beijing, China) according to the manufacturer's protocol. Splenocytes (1×10^6) were cultured in a 24-well culture plate (Corning, NY, USA) in the presence or absence

of 10^5 PFU of purified UV-RSV. The culture plate was maintained in a 5% CO_2 incubator at 37°C for 72 h, and the supernatants were then collected and stored at -80°C for subsequent assays. For lung cytokine detection, lung tissues were collected on Day 4 postchallenge (p.c.) and homogenized. After centrifugation, the supernatants were collected and stored at -80°C for the subsequent assay. Th1 (IFN-γ, IL-2), Th2 (IL-4, IL-5), IL-10 and IL-17A cytokines present in the supernatants were quantitatively measured using commercially available ELISA kits (Bio Legend, Camarillo, CA, USA).

Antibody binding to purified VLPs was performed as previously described (49). Briefly, equivalent amounts of Pre-F or Post-F VLPs were added directly to the microtiter wells (1 µg of total VLP protein in 100 µl) and incubated at 37°C for 16 h. After washing thrice with PBS, different concentrations of selected antibody (anti-F131-2A or anti-F D25) were added to each well and then incubated for 2 h at room temperature (RT). After three washes in PBS, the secondary antibody (goat anti-mouse IgG-HRP or goat anti-human IgG-HRP) diluted with PBS containing 1% BSA was added to each well (100 µl/well) and then incubated at RT for 1.5 h. TMB (3,3',5,5'-tetramethylbenzidine; Sigma) substrate in a 100 µl volume was added to each well. After 15 to 20 min of incubation at RT, the reaction was stopped by adding 100 µl of 2 M H_2SO_4 to each well, and the optical density at 450 nm was measured using an ELISA reader (Multidkan MK3; Thermo Fisher Scientific).

RSV immunoplaque and neutralization antibody assays

RSV neutralizing antibody titres were determined by a plaque reduction assay as previously described (18, 39). Briefly, mouse sera were inactivated at 56°C for 30 min and then serially diluted 2-fold in DMEM. Purified RSV was diluted to approximately 100 PFU in 100 µl and added to the diluted sera in 100-µl aliquots. The virus-serum mixture or a virus-DMEM control was incubated at 37°C for 1 h. Then, the mixture was added to prewashed Vero cells in 24-well plates. After 2 h of

incubation, the mixture was removed, and 1 ml of methylcellulose overlay (1 volume of 2 ×DMEM containing 4% FBS, 2% penicillin streptomycin, and 1 volume of 2% methylcellulose) was added to each well. The plates were incubated at 37°C for 3 to 5 days, and the plaques were stained as previously described (39). The neutralization titre was defined as the $\log_2$ of the reciprocal of the highest dilution of serum that reduced the virus titre by 50%.

Quantitative real-time (qRT)-PCR

RSV load in the lung was quantified by qRT–PCR (18). Total RNA of lung tissues was extracted using RNA Pure reagent (Aidlab, Beijing, China) and reverse transcribed into cDNA using a reverse transcription kit (Toyoba, Osaka, Japan) according to the manufacturer's instructions. RSV N gene copies were quantified using 2×SYBR green master mix (Novoprotein, Shanghai, China) in a 7500 Real-Time PCR System (Applied Biosystems, USA). The qRT–PCR primer sequences are listed in Table 1.

Flow cytometry

Cytokine staining was performed as previously described (13, 18, 50). Lung cells were surface-stained with mAbs specific to CD4-FITC (Clone RM4-5) and CD25-APC (Clone PC61) (BioLegend, San Diego, CA). After fixation and permeabilization, the cells were intracellularly stained with PE-labelled anti-mouse Foxp3 (Clone MF-14) or IL17A mAb (Clone TC11-18H10.1) (BioLegend). Then, the stained cells were analyzed by flow cytometry (Beckman Coulter CytoFlex, USA). Data were analysed using CytoFlex software and are presented as the percentage of $CD25^+ Foxp3^+$ cells or IL17A-producing cells among $CD4^+$ T cells. All gating strategies are specified in the Supplementary Figure S1.

Statistical analysis

Comparisons of various groups were accomplished by Student's t tests or analysis of variance (ANOVA) followed by the Tukey test or nonparametric Kruskal–Wallis test. A P value of less than 0.05 was considered statistically significant.

Results

Preparation and characterization of chimeric VLPs

Recombinant baculovirus was constructed as described in the Materials and Methods section (Figure 1A). Pre-F or Post-F VLPs were produced by Sf9 cells infected simultaneously with rBV-RSV-Pre-F and rBV-IAV-M1 or rBV-RSV-Post-F and rBV-IAV-M1, respectively. After 72 h of culture, the resultant supernatants of infected Sf9 cells were harvested for analysis of F and M1 expression by western blotting. The data showed that the engineered Pre-F, Post-F or IAV M1 protein could be expressed efficiently from infected Sf9 cells and that the expected molecular weights of RSV F (~63 kDa) and IAV M1 (~28 kDa) proteins were successfully detected (Figure 1B). SDS−PAGE analysis showed that the prepared VLPs contained highly pure F and M1 proteins (Figure 2A). Spherical self-assembling VLPs ~50-100 nm in diameter were observed under an electron microscope (Figure 2B). These data demonstrated that VLPs were successfully generated from rBV-infected Sf9 cells.

Previous studies and clinical observations in human sera demonstrated that RSV neutralizing antibodies are specific to the prefusion structure (22, 24, 26). To characterize the RSV Pre-F or Post-F form in the VLPs, the characteristic antigenic sites Ø and I based on the Pre-F and Post-F conformations were detected using the specific mAbs D25 and 131-2A, respectively. The data showed that mAb D25 bound effectively to VLPs containing Pre-F conformation with antigenic site Ø (Figure 2C, left). In contrast, mAb 131-2A bound strongly to VLPs containing the Post-F conformation with antigenic site I (Figure 2C, right). The results identified that the VLPs generated from rBV-Sf9 cells contained specifically antigenic sites Ø and I of the Pre-F and Post-F conformations, respectively.

Antibody and cytokine responses in mice induced by Pre-F and Post-F VLPs

RSV-specific IgG, IgG2a, and IgG1 concentrations in the sera of immunized mice were detected by ELISA. Compared with the Post-F VLPs, the Pre-F VLPs induced significantly increased RSV-specific IgG and IgG2a antibody levels ($P < 0.05$), but a similar IgG1 antibody level was observed ($P > 0.05$) (Figure 3A). Vaccination with the Pre-F VLPs and Post-F VLPs elicited Th1-dominant responses with median IgG2a/IgG1 ratios of 1.22 and 1.13, respectively; in contrast, immunization with UV-RSV resulted in a Th2-biased response with an IgG2a/IgG1 ratio of 0.94 (Figure 3B). Vaccination with Pre-F VLPs induced a higher ratio of IgG2a antibodies than vaccination with UV-RSV or Post-F VLPs. Sera of vaccinated mice exhibited stronger binding ability with the corresponding VLPs (Supplementary Figure S2). Analysis of RSV neutralizing antibody (NAb) in the sera of vaccinated mice showed that although both Pre-F VLPs and Post-F VLPs induced RSV NAb production, Pre-F VLPs elicited significantly increased RSV NAb levels compared with Post-F VLPs ($P < 0.01$) (Figure 3C).

To investigate cellular immune responses, we examined Th1-type (IFN-γ and IL-2) and Th2-type (IL-4 and IL-5) cytokines in the splenocyte supernatants of vaccinated mice. In the PBS-treated
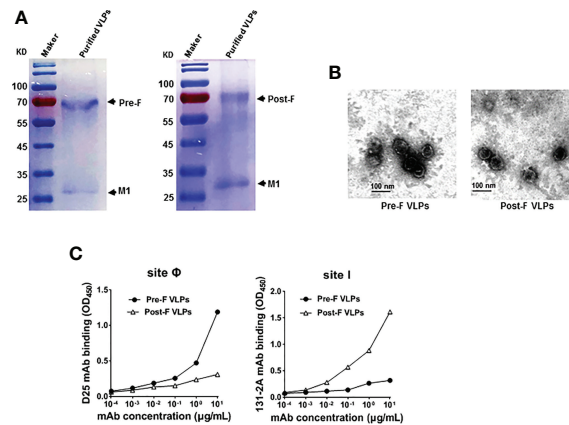
FIGURE 2

Purification and characterization of Pre-F VLPs and Post-F VLPs. **(A)** Purified proteins were subjected to 12% SDS–PAGE and stained with Coomassie blue. M, Molecular marker; Lane 1, Pre-F VLPs; Lane 2, Post-F VLPs. **(B)** Electron microscopic analysis of Pre-F VLPs and Post-F VLPs. Scale bar, 100 nm. **(C)** Monoclonal antibody specifically binding to purified VLPs. Pre-F and Post-F VLPs containing equivalent amounts of F protein, as determined using mAb D25 or mAb 131-2A as the primary antibody and goat anti-human IgG-HRP for D25 (left) or goat anti-mouse IgG-HRP for 131-2A (right) as the secondary antibody, respectively. Antibodies and sites are indicated in the figure. OD, optical density.

group, both Th1-type (IFN-γ and IL-2) and Th2-type (IL-4 and IL-5) cytokines displayed very low concentrations. Compared with the VLP-vaccinated groups, significantly increased levels of Th1-type and Th2-type cytokines were induced by UV-RSV. However, in the VLP-vaccinated mice, the levels of the cytokines IFN-γ and IL-2 were only reduced approximately 1.4-fold, and the levels of the cytokines IL-4 and IL-5 were reduced ~2-fold and ~ 4-fold, respectively (Figure 4). Importantly, compared with Post-F VLPs, vaccination with Pre-F VLPs induced significantly increased Th1 type and decreased Th2-type cytokine production (Figure 4). Without RSV stimulation, both Th1-type and Th2-type cytokines were almost undetectable (Figure 4). Our data demonstrated that Pre-F VLPs elicited a mixed Th1/Th2 response with Th1-biased cellular immunity to RSV.

CD4$^+$ T-cell subsets and cytokine profiles in the lungs of vaccinated mice following RSV infection.

Distinct CD4$^+$ T-cell subsets and Th2-type cytokines play crucial roles in RSV vaccine-enhanced immunopathology (13, 14, 47, 51). We further investigated CD4$^+$CD25$^+$Foxp3$^+$ Treg and IL-17A-producing CD4$^+$ T-cell subsets and the representative cytokines in the lungs of vaccinated mice following RSV challenge. The data showed that the percentage of CD4$^+$CD25$^+$Foxp3$^+$ Treg cells in VLP-vaccinated mice was significantly increased compared to that in UV-RSV-immunized mice ($P <0.001$) (Figure 5A). In contrast, significantly decreased IL-17A$^+$-producing CD4$^+$ T cells were observed in VLP-vaccinated mice compared to UV-RSV-immunized mice ($P < 0.01$)
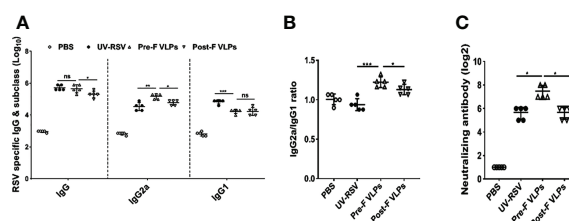

FIGURE 3

VLPs elicited humoral immune responses in mice. Groups of five BALB/c mice were inoculated with 10 μg of Pre-F VLPs, Post-F VLPs, 1×10^5 PFU of purified UV-inactivated RSV or 100 μl PBS following i.m. inoculation. Mice in all groups received a booster twice in 2-week intervals with the same amount of inoculum. Sera were collected at 2 weeks after the final immunization to determine RSV-specific IgG, IgG2a, and IgG1 titres *via* ELISA **(A, B)** and neutralization antibody (NAb) titres *via* the neutralization assay **(C)**. Data are expressed as the GMT (geometric mean titre) of five mice. *P* values were calculated with one-way ANOVA or Student's *t* test followed by the Tukey test. ***P < 0.001; **P < 0.01; *P < 0.05; ns, not significant.
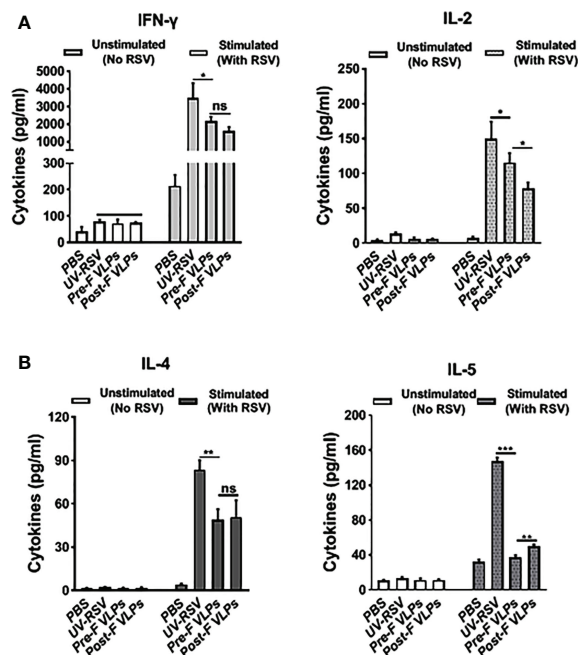
FIGURE 4
VLPs elicited cellular immune responses in mice. Spleen cells were isolated at 2 weeks after the last immunization and stimulated with 1×10^5 PFU of purified UV-inactivated RSV. The supernatants were collected after 72 h of incubation, and Th1 cytokines (IFN-γ and IL-2) **(A)** and Th2 cytokines (IL-4 and IL-5) **(B)** concentrations were measured by ELISA. All data are presented as the mean values ($\pm$ SD) from five mice in each group. P values were calculated with one-way ANOVA or Student's *t test* followed by the Tukey test. ***$P < 0.001$; **$P < 0.01$; *$P < 0.05$; ns, not significant.

(Figure 5B). In particular, a significantly increased percentage of CD4$^+$CD25$^+$Foxp3$^+$ Treg cells ($P < 0.01$) (Figure 5A) and a significantly decreased amount of IL-17A$^+$-producing CD4$^+$ T cells ($P < 0.05$) (Figure 5B) were observed in mice vaccinated with Pre-F VLPs compared to mice vaccinated with Post-F VLPs. Similar concentrations of the pulmonary cytokines IFN-γ, IL-2, IL-5 and IL-17A were observed in mice vaccinated with Pre-F compared with Post-F VLPs Figure 5C. Importantly, significantly decreased concentrations of the Th2-type cytokines IL-4 ($P < 0.05$) and IL-5 ($P < 0.001$) and significantly increased production of the Treg cell-related cytokine IL-10 ($P < 0.01$) were observed in VLP-vaccinated mice compared to UV-RSV-immunized mice Figure 5C. Interestingly, compared to Post-F VLPs, vaccination of Pre-F VLPs elicited significantly decreased IL-4 ($P < 0.01$) and increased IL-10 secretion ($P < 0.05$) (Figure 5C). Our results indicated that Pre-F VLPs elicited balanced Treg/Th17 responses in vaccinated mice upon subsequent RSV infection.

Pulmonary viral load and pathology in mice vaccinated with VLPs following RSV infection

To investigate the immune protection induced by the VLPs, the RSV load in the lungs of vaccinated mice was quantified on Day 4 p.c. by qRT−PCR. As a control, the high RSV N gene copy numbers (~ 10^6 copies/100 ng total RNA) were detected in the lungs of PBS-treated mice, whereas very low RSV N gene copy numbers (~ 10^3 copies) (approximate background value of test) were observed in the lungs of mice vaccinated with VLPs (Figure 6A), demonstrating that vaccination with Pre-F VLPs or Post-F VLPs effectively inhibited RSV replication in the lungs of mice.

We further investigated pathological injury in the lungs of vaccinated mice after RSV infection. The data showed that mice immunized with UV-RSV exhibited severe lung pathology, including extensive lymphocyte infiltration around the blood vessels and alveolar hemorrhage. In contrast, mice vaccinated with VLPs displayed signs of mild inflammation in the lungs. Importantly, mice vaccinated with Pre-F VLPs presented similar histological features to naive mice in the lungs (Figure 6B). After RSV infection, the average inflammation severity scores of vaccinated mice were in the following order: UV-RSV > PBS > Post-F VLPs > Pre-F VLPs (Table 2). Data from PAS staining showed that overt inflammation and mucus hypersecretion (black arrows) were observed in the lungs of UV-RSV-immunized mice and mild mucus accumulation was observed in the lungs of Post-F VLP-immunized mice (Figure 6C). However, no mucus secretion was observed in the lungs of mice vaccinated with Pre-F VLPs,
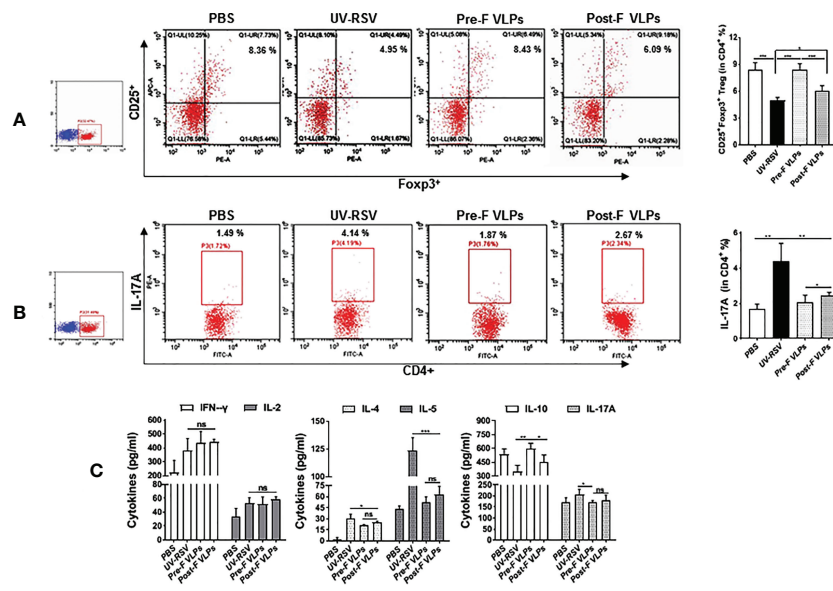
FIGURE 5

Cellular immune responses in the lungs of vaccinated mice induced by RSV challenge infection. Mice were immunized i.m. thrice and challenged i.n. with RSV 2 weeks after the final immunization. Lungs were harvested on Day 4 p.c. The percentage of CD25+ Foxp3+ Treg cells **(A)** or IL-17A **(B)** in CD4+ T cells from the lungs was measured by flow cytometry with specific antibody staining. **(C)** Th1 cytokine (IFN-γ & IL-2), Th2 cytokine (IL-4 & IL-5) and the cytokines IL-10 and IL-17A concentrations were measured by ELISA. Data are presented as mean values ± SDs for six mice in each group. Pairwise comparisons of values were performed using one-way ANOVA or Student's t test followed by the Tukey test. ***P < 0.001; **P < 0.01; *P < 0.05; ns, not significant.

FIGURE 6

RSV load and histopathological analysis of lung tissues from vaccinated mice upon RSV challenge. Mice were immunized i.m. thrice and challenged i.n. with RSV 2 weeks after the final immunization. Lungs were harvested on Day 4 p.c. **(A)** RSV copy numbers in lung tissues were measured by qRT–PCR. Data are presented as mean values ± SDs for six mice in each group. Pairwise comparisons of values were performed using one-way ANOVA followed by the Tukey test. ***P < 0.001; **P < 0.01; *P < 0.05; ns, not significant. **(B, C)** Representative h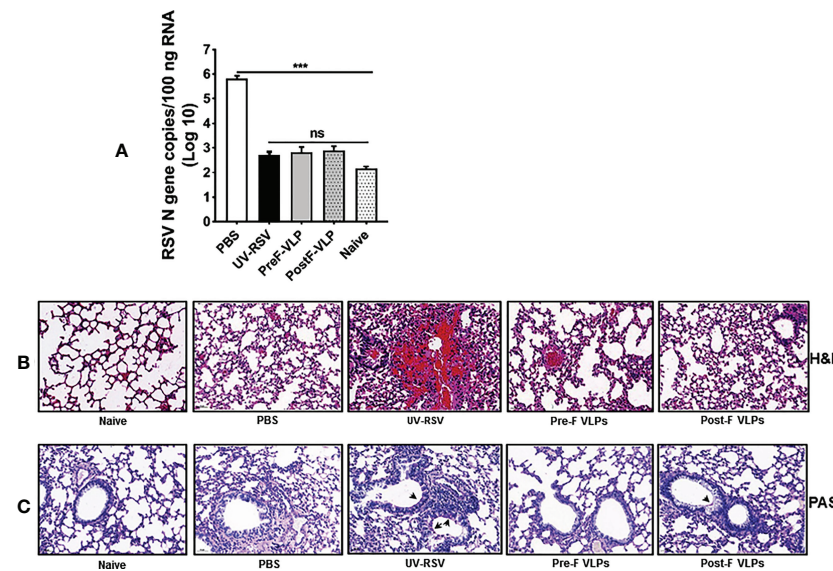istopathological section of lung from immunized mice at Day 4 after RSV challenge by haematoxylin-eosin (H&E) **(B)** and periodic acid-Schiff (PAS) staining **(C)** for each experimental group.

TABLE 2   Histopathological scores of lungs from immunized mice on Day 4 following RSV challenge.

Inoculum	Histopathological score[a]			
	Alveolartissue[b]	Peribronchial aggregation[c]	Perivascular aggregation[d]	Mucus[e]
Naive	0	0	0	1
PBS	2 ± 0.16	2.2 ± 0.16	2.27 ± 0.19	1.33 ± 0.09
UV-RSV	3.67 ± 0.09	3.67 ± 0.09	3.53 ± 0.09	2.6 ± 0.16
Pre-F VLPs	0.67 ± 0.09	0.73 ± 0.09	0.8 ± 0.16	1.13 ± 0.09
Post-F VLPs	1.33 ± 0.09	1.53 ± 0.25	1.53 ± 0.09	1.4 ± 0.16

[a]The lung inflammation severity scores were defined on a scale from 0 to 4 according to the H&E-stained sections as follows: 0-inflammation was not present, 1- minimal inflammation, 2-mild inflammation, 3-moderate inflammation, and 4-marked inflammation. Scores of mucus production scale according to the PAS-stained sections as follows: 1-no mucus detectable, 2-rare mucus, 3-moderate mucus accumulation, and 4-severe mucus accumulation. Data represent the mean values ± SDs (n = 3).
[b]Alveolar tissue: Pre-F VLPs vs. Post-F VLPs (p < 0.01).
[c]Peribronchial aggregation: Pre-F VLPs vs. Post-F VLPs (p < 0.05).
[d]Perivascular aggregation: Pre-F VLPs vs. Post-F VLPs (p < 0.05).
[e]Mucus: Pre-F VLPs vs. Post-F VLPs (p > 0.05).

which was similar to the characteristics of naive mice. These results revealed that vaccination with Pre-F VLPs induced effective protection against RSV infection without enhanced pulmonary immunopathology in mice.

Discussion

A licensed vaccine for RSV is not currently available despite the fact that RSV is the major cause of lower respiratory tract infections in children. Vaccine-enhanced immunopathology has significantly hampered the development of an RSV vaccine. Previous studies have shown that poorly neutralizing antibodies, a Th2-biased immune response and distinct CD4^{+} T-cell subsets correlate with VED upon RSV infection (12, 13, 47, 52) and that high neutralizing antibody levels correlate with the prevention of disease severity and a lower risk of infection (6, 53, 54). Therefore, induction of a high-affinity neutralizing antibody and a balanced immune response should be preferentially considered for the design of a safe and effective RSV vaccine (18, 55).

Experimental studies and clinical observations in human sera demonstrated that RSV neutralizing antibodies are specific to the prefusion structure (22, 24, 26). Structure-based design of vaccines showed that a highly stable prefusion F conformation would be a promising subunit vaccine candidate against RSV (27, 29). Following immunization of mice, VLPs containing the stabilized Pre-F configuration from Newcastle disease virus (NDV) induced significantly higher neutralizing antibody titres than the Post-F VLPs or wild-type F VLPs after a single immunization (49). As a well-known tool for the production of subunit vaccines, the rBV-Sf9 insect cell expression system has been widely employed (56–58). VLPs containing the RSV F protein

generated by rBV-Sf9 cells confer effective protection against RSV infection (37, 38). In the present study, we successfully produced influenza M1-based VLPs containing RSV Pre-F or Post-F configuration using the rBV-Sf9 cell expression system. We further characterized the assembly and immunological properties of these VLPs. Our results confirmed that the Pre-F and Post-F VLPs generated from rBV-Sf9 cells displayed specific antigenic sites Ø and I, respectively. The antigenic site Ø was the crucial target site recognized by RSV-neutralizing antibodies, and the postfusion form of the F protein led to the lack of specific epitopes Ø (22, 26, 27). Antigenic site I was more pronounced on Post-F, and site I-directed antibodies are typically nonneutralizing (59). Our results demonstrated that Pre-F VLPs elicited significantly increased RSV-specific neutralizing antibody titres compared to PostF VLPs or UV-RSV. The high level of Pre-F specific antibodies in human sera play an important role in alleviating antibody-dependent disease enhancement (60–62).

In our study, immunization with both Pre-F and Post-F VLPs predominantly induced IgG2a isotype antibodies and Th1-associated cytokines (IFN-γ and IL-2) and significantly decreased Th2-biased cytokine responses (IL-4 and IL-5) compared with UV-RSV. For cytokine secretion in the lungs of mice vaccinated with VLPs, significantly decreased IL-4, IL-5, and IL-17A and increased IL-10 cytokines were observed compared to UV-RSV. Importantly, compared with Post-F VLPs, Pre-F VLPs elicited a significantly increased IgG2a/IgG1 ratio and high RSV neutralizing antibody levels and significantly decreased IL-5 secretion. However, both Pre-F VLPs and Post-F VLPs induced similar IFN-γ and IL-4 cytokine levels (Figure 4). We further tested the Treg and Th17 subsets in the lungs of vaccinated mice. Compared to UV-RSV, vaccination with RSV F VLPs upregulated the percentage of Treg (CD4^{+}CD25^{+}FoxP3^{+}) cells and downregulated the percentage of Th17 (CD4^{+}IL-17A^{+})

cells. Significantly increased Treg cells and decreased Th17 cells were observed in the lungs of mice vaccinated with Pre-F VLPs compared with Post-F VLPs. During RSV infection, Treg cells functionally regulate the immunological environment to avoid excessive inflammatory T-cell responses and aid in limiting inefficient Th2-type immune responses (55). Therefore, Treg cells play a pivotal role in alleviating vaccine-enhanced immunopathology in RSV infection (55, 63). In contrast, Th17 cells are functionally considered to exacerbate inflammatory diseases, including chronic pulmonary obstruction, cystic fibrosis, and asthma (64), and are involved in increasing mucus secretion and reducing viral clearance (65). A current study showed that vaccination with commercial PreF protein formulated with a Th1/Th2-balanced adjuvant induced suppression of RSV replication and inhibited airway eosinophilia and mucus accumulation in mice (66). Additionally, poor avidity and affinity maturation caused nonprotective antibody development and Th2-associated immunopathology (52). As expected, our results demonstrated that a high neutralizing antibody level and a Th1/Th2-balanced immune response were induced by Pre-F VLPs, resulting in alleviation of pulmonary pathology and airway mucus secretion in vaccinated mice.

VLPs containing RSV F and/or G proteins have been intensively investigated using different vaccine platforms (18, 37, 39, 40, 44, 67). For NDV-RSV VLPs, the potential contamination of mammalian DNA and other deleterious factors from sera and/or cells require removal from VLPs (49, 68). The rBV-produced VLPs from serum-free insect cell cultures are beneficial to VLP vaccine technology. RSV VLP production utilizing the rBV-insect cell expression system is FDA approved for human use, and the high levels of VLPs generated from suspension cultures of insect cells will facilitate large-scale vaccine production (57, 58, 69). Therefore, the work presented in this study provides a novel, promising strategy for the development of RSV vaccine candidates.

Data availability statement

The original contributions presented in the study are included in the article/supplementary materials, further inquiries can be directed to the corresponding author/s.

Ethics statement

The animal study was reviewed and approved by the Institutional Animal Care and Use Committee of Wuhan University.

Author contributions

ZP, JL, and LL designed and conceived the study. JL, HQ, WL, and RL conducted the experiments. ZP, JL, and LL analyzed the data and wrote the manuscript. All authors contributed to the article and approved the submitted version.

Funding

Conflict of interest

The authors declare that the research was conducted in the absence of any commercial or financial relationships that could be construed as a potential conflict of interest.

Publisher's note

All claims expressed in this article are solely those of the authors and do not necessarily represent those of their affiliated organizations, or those of the publisher, the editors and the reviewers. Any product that may be evaluated in this article, or claim that may be made by its manufacturer, is not guaranteed or endorsed by the publisher.

Supplementary material

The Supplementary Material for this article can be found online at: https://www.frontiersin.org/articles/10.3389/fimmu. 2022.1054005/full#supplementary-material

References

1. Blount RE Jr., Morris JA, Savage RE. Recovery of cytopathogenic agent from chimpanzees with coryza. *Proc Soc Exp Biol Med* (1956) 92(3):544–9. doi: 10.3181/00379727-92-22538

2. Chanock R, Finberg L. Recovery from infants with respiratory illness of a virus related to chimpanzee coryza agent (Cca). ii. epidemiologic aspects of infection in infants and young children. *Am J Hyg* (1957) 66(3):291–300. doi: 10.1093/oxfordjournals.aje.a119902

3. Boyoglu-Barnum S, Chirkova T, Anderson LJ. Biology of infection and disease pathogenesis to guide rsv vaccine development. *Front Immunol* (2019) 10:1675. doi: 10.3389/fimmu.2019.01675

4. Li Y, Wang X, Blau DM, Caballero MT, Feikin DR, Gill CJ, et al. Global, regional, and national disease burden estimates of acute lower respiratory infections due to respiratory syncytial virus in children younger than 5 years in 2019: A systematic analysis. *Lancet* (2022) 399(10340):2047–64. doi: 10.1016/S0140-6736(22)00478-0

5. Chatterjee A, Mavunda K, Krilov LR. Current state of respiratory syncytial virus disease and management. *Infect Dis Ther* (2021) 10(Suppl 1):5–16. doi: 10.1007/s40121-020-00387-2

6. Glezen WP, Taber LH, Frank AL, Kasel JA. Risk of primary infection and reinfection with respiratory syncytial virus. *Am J Dis Child* (1986) 140(6):543–6. doi: 10.1001/archpedi.1986.02140200053026

7. Henderson FW, Collier AM, Clyde WAJr., Denny FW. Respiratory-Syncytial-Virus infections, reinfections and immunity. a prospective, longitudinal study in young children. *N Engl J Med* (1979) 300(10):530–4. doi: 10.1056/NEJM197903083001004

8. Fulginiti VA, Eller JJ, Sieber OF, Joyner JW, Minamitani M, Meiklejohn G. Respiratory virus immunization. i. a field trial of two inactivated respiratory virus vaccines; an aqueous trivalent parainfluenza virus vaccine and an alum-precipitated respiratory syncytial virus vaccine. *Am J Epidemiol* (1969) 89 (4):435–48. doi: 10.1093/oxfordjournals.aje.a120956

9. Kapikian AZ, Mitchell RH, Chanock RM, Shvedoff RA, Stewart CE. An epidemiologic study of altered clinical reactivity to respiratory syncytial (Rs) virus infection in children previously vaccinated with an inactivated rs virus vaccine. *Am J Epidemiol* (1969) 89(4):405–21. doi: 10.1093/oxfordjournals.aje.a120954

10. Kim HW, Canchola JG, Brandt CD, Pyles G, Chanock RM, Jensen K, et al. Respiratory syncytial virus disease in infants despite prior administration of antigenic inactivated vaccine. *Am J Epidemiol* (1969) 89(4):422–34. doi: 10.1093/oxfordjournals.aje.a120955

11. Ruckwardt TJ, Morabito KM, Graham BS. Immunological lessons from respiratory syncytial virus vaccine development. *Immunity* (2019) 51(3):429–42. doi: 10.1016/j.immuni.2019.08.007

12. Waris ME, Tsou C, Erdman DD, Zaki SR, Anderson LJ. Respiratory synctial virus infection in Balb/C mice previously immunized with formalin-inactivated virus induces enhanced pulmonary inflammatory response with a predominant Th2-like cytokine pattern. *J Virol* (1996) 70(5):2852–60. doi: 10.1128/jvi.70.5.2852-2860.1996

13. Zhao Y, Ma C, Yang J, Zou X, Pan Z. Dynamic host immune and transcriptomic responses to respiratory syncytial virus infection in a vaccination-challenge mouse model. *Virol Sin* (2021) 36(6):1327–40. doi: 10.1007/s12250-021-00418-3

14. Connors M, Giese NA, Kulkarni AB, Firestone CY, Morse HC3rd, Murphy BR. Enhanced pulmonary histopathology induced by respiratory syncytial virus (Rsv) challenge of formalin-inactivated rsv-immunized Balb/C mice is abrogated by depletion of interleukin-4 (Il-4) and il-10. *J Virol* (1994) 68(8):5321–5. doi: 10.1128/JVI.68.8.5321-5325.1994

15. Graham BS. Biological challenges and technological opportunities for respiratory syncytial virus vaccine development. *Immunol Rev* (2011) 239 (1):149–66. doi: 10.1111/j.1600-065X.2010.00972.x

16. Mok H, Lee S, Utley TJ, Shepherd BE, Polosukhin VV, Collier ML, et al. Venezuelan Equine encephalitis virus replicon particles encoding respiratory syncytial virus surface glycoproteins induce protective mucosal responses in mice and cotton rats. *J Virol* (2007) 81(24):13710–22. doi: 10.1128/JVI.01351-07

17. Zhang Y, Qiao L, Hu X, Zhao K, Zhang Y, Chai F, et al. Baculovirus vectors expressing f proteins in combination with virus-induced signaling adaptor (Visa) molecules confer protection against respiratory syncytial virus infection. *Vaccine* (2016) 34(2):252–60. doi: 10.1016/j.vaccine.2015.11.027

18. Yang J, Ma C, Zhao Y, Fan A, Zou X, Pan Z. Hepatitis b virus core particles containing a conserved region of the G protein combined with interleukin-35 protected mice against respiratory syncytial virus infection without vaccine-enhanced immunopathology. *J Virol* (2020) 94(13):e00007–20. doi: 10.1128/JVI.00007-20

19. Zhan X, Hurwitz JL, Krishnamurthy S, Takimoto T, Boyd K, Scroggs RA, et al. Respiratory syncytial virus (Rsv) fusion protein expressed by recombinant Sendai virus elicits b-cell and T-cell responses in cotton rats and confers protection against rsv subtypes a and b. *Vaccine* (2007) 25(52):8782–93. doi: 10.1016/j.vaccine.2007.10.038

20. Kohlmann R, Schwannecke S, Tippler B, Ternette N, Temchura VV, Tenbusch M, et al. Protective efficacy and immunogenicity of an adenoviral vector vaccine encoding the codon-optimized f protein of respiratory syncytial virus. *J Virol* (2009) 83(23):12601–10. doi: 10.1128/JVI.01036-09

21. Olmsted RA, Elango N, Prince GA, Murphy BR, Johnson PR, Moss B, et al. Expression of the f glycoprotein of respiratory syncytial virus by a recombinant vaccinia virus: Comparison of the individual contributions of the f and G glycoproteins to host immunity. *Proc Natl Acad Sci USA* (1986) 83(19):7462–6. doi: 10.1073/pnas.83.19.7462

22. McLellan JS, Chen M, Leung S, Graepel Kevin W, Du X, Yang Y, et al. Structure of rsv fusion glycoprotein trimer bound to a prefusion-specific neutralizing antibody. *Science* (2013) 340(6136):1113–7. doi: 10.1126/science.1234914

23. Swanson Kurt A, Settembre Ethan C, Shaw Christine A, Dey Antu K, Rappuoli R, Mandl Christian W, et al. Structural basis for immunization with postfusion respiratory syncytial virus fusion f glycoprotein (Rsv f) to elicit high neutralizing antibody titers. *Proc Natl Acad Sci* (2011) 108(23):9619–24. doi: 10.1073/pnas.1106536108

24. Corti D, Bianchi S, Vanzetta F, Minola A, Perez L, Agatic G, et al. Cross-neutralization of four paramyxoviruses by a human monoclonal antibody. *Nature* (2013) 501(7467):439–43. doi: 10.1038/nature12442

25. Wen X, Mousa JJ, Bates JT, Lamb RA, Crowe JEJr., Jardetzky TS. Structural basis for antibody cross-neutralization of respiratory syncytial virus and human metapneumovirus. *Nat Microbiol* (2017) 2:16272. doi: 10.1038/nmicrobiol.2016.272

26. Magro M, Mas V, Chappell K, Vázquez M, Cano O, Luque D, et al. Neutralizing antibodies against the preactive form of respiratory syncytial virus fusion protein offer unique possibilities for clinical intervention. *Proc Natl Acad Sci* (2012) 109(8):3089–94. doi: 10.1073/pnas.1115941109

27. McLellan JS, Chen M, Joyce MG, Sastry M, Stewart-Jones GBE, Yang Y, et al. Structure-based design of a fusion glycoprotein vaccine for respiratory syncytial virus. *Science* (2013) 342(6158):592–8. doi: 10.1126/science.1243283

28. Joyce MG, Zhang B, Ou L, Chen M, Chuang G-Y, Druz A, et al. Iterative structure-based improvement of a fusion-glycoprotein vaccine against rsv. *Nat Struct Mol Biol* (2016) 23(9):811–20. doi: 10.1038/nsmb.3267

29. Krarup A, Truan D, Furmanova-Hollenstein P, Bogaert L, Bouchier P, Bisschop IJM, et al. A highly stable prefusion rsv f vaccine derived from structural analysis of the fusion mechanism. *Nat Commun* (2015) 6:8143. doi: 10.1038/ncomms9143

30. Crank Michelle C, Ruckwardt Tracy J, Chen M, Morabito Kaitlyn M, Phung E, Costner Pamela J, et al. A proof of concept for structure-based vaccine design targeting rsv in humans. *Science* (2019) 365(6452):505–9. doi: 10.1126/science.aav9033

31. Marcandalli J, Fiala B, Ols S, Perotti M, de van der Schueren W, Snijder J, et al. Induction of potent neutralizing antibody responses by a designed protein nanoparticle vaccine for respiratory syncytial virus. *Cell* (2019) 176(6):1420–31.e17. doi: 10.1016/j.cell.2019.01.046

32. Steff AM, Monroe J, Friedrich K, Chandramouli S, Nguyen TL, Tian S, et al. Pre-fusion rsv f strongly boosts pre-fusion specific neutralizing responses in cattle pre-exposed to bovine rsv. *Nat Commun* (2017) 8(1):1085. doi: 10.1038/s41467-017-01092-4

33. Jennings GT, Bachmann MF. The coming of age of virus-like particle vaccines. *Biol Chem* (2008) 389(5):521–36. doi: 10.1515/bc.2008.064

34. Mena JA, Kamen AA. Insect cell technology is a versatile and robust vaccine manufacturing platform. *Expert Rev Vaccines* (2011) 10(7):1063–81. doi: 10.1586/erv.11.24

35. Mohsen MO, Bachmann MF. Virus-like particle vaccinology, from bench to bedside. *Cell Mol Immunol* (2022) 19(9):993–1011. doi: 10.1038/s41423-022-00897-8

36. Roldao A, Mellado MC, Castilho LR, Carrondo MJ, Alves PM. Virus-like particles in vaccine development. *Expert Rev Vaccines* (2010) 9(10):1149–76. doi: 10.1586/erv.10.115

37. Quan FS, Kim Y, Lee S, Yi H, Kang SM, Bozja J, et al. Viruslike particle vaccine induces protection against respiratory syncytial virus infection in mice. *J Infect Dis* (2011) 204(7):987–95. doi: 10.1093/infdis/jir474

38. Kim KH, Lee YT, Hwang HS, Kwon YM, Kim MC, Ko EJ, et al. Virus-like particle vaccine containing the f protein of respiratory syncytial virus confers protection without pulmonary disease by modulating specific subsets of dendritic cells and effector T cells. *J Virol* (2015) 89(22):11692–705. doi: 10.1128/jvi.02018-15

39. Murawski MR, McGinnes LW, Finberg RW, Kurt-Jones EA, Massare MJ, Smith G, et al. Newcastle Disease virus-like particles containing respiratory syncytial virus G protein induced protection in Balb/C mice, with no evidence of immunopathology. *J Virol* (2010) 84(2):1110–23. doi: 10.1128/JVI.01709-09

40. McGinnes LW, Gravel KA, Finberg RW, Kurt-Jones EA, Massare MJ, Smith G, et al. Assembly and immunological properties of Newcastle disease virus-like particles containing the respiratory syncytial virus f and G proteins. *J Virol* (2011) 85(1):366–77. doi: 10.1128/jvi.01861-10

41. Blanco JCG, Pletneva LM, McGinnes-Cullen L, Otoa RO, Patel MC, Fernando LR, et al. Efficacy of a respiratory syncytial virus vaccine candidate in a maternal immunization model. *Nat Commun* (2018) 9(1):1904. doi: 10.1038/s41467-018-04216-6

42. Cullen LM, Schmidt MR, Morrison TG. The importance of rsv f protein conformation in vlps in stimulation of neutralizing antibody titers in mice

previously infected with rsv. *Hum Vaccin Immunother* (2017) 13(12):2814–23. doi: 10.1080/21645515.2017.1329069

43. Yoshida S, Kondoh D, Arai E, Matsuoka H, Seki C, Tanaka T, et al. Baculovirus virions displaying plasmodium berghei circumsporozoite protein protect mice against malaria sporozoite infection. *Virology* (2003) 316(1):161–70. doi: 10.1016/j.virol.2003.08.003

44. Qiao L, Zhang Y, Chai F, Tan Y, Huo C, Pan Z. Chimeric virus-like particles containing a conserved region of the G protein in combination with a single peptide of the M2 protein confer protection against respiratory syncytial virus infection. *Antiviral Res* (2016) 131:131–40. doi: 10.1016/j.antiviral.2016.05.001

45. Cullen LM, Schmidt MR, Torres GM, Capoferri AA, Morrison TG. Comparison of immune responses to different versions of vlp associated stabilized rsv pre-fusion f protein. *Vaccines (Basel)* (2019) 7(1):21. doi: 10.3390/vaccines7010021

46. Zhang L, Durr E, Galli JD, Cosmi S, Cejas PJ, Luo B, et al. Design and characterization of a fusion glycoprotein vaccine for respiratory syncytial virus with improved stability. *Vaccine* (2018) 36(52):8119–30. doi: 10.1016/j.vaccine.2018.10.032

47. Knudson CJ, Hartwig SM, Meyerholz DK, Varga SM. Rsv vaccine-enhanced disease is orchestrated by the combined actions of distinct Cd4 T cell subsets. *PloS Pathog* (2015) 11(3):e1004757. doi: 10.1371/journal.ppat.1004757

48. Chung YC, Ho MS, Wu JC, Chen WJ, Huang JH, Chou ST, et al. Immunization with virus-like particles of enterovirus 71 elicits potent immune responses and protects mice against lethal challenge. *Vaccine* (2008) 26(15):1855–62. doi: 10.1016/j.vaccine.2008.01.058

49. McGinnes CL, Schmidt MR, Kenward SA, Woodland RT, Morrison TG. Murine immune responses to virus-like particle-associated pre- and postfusion forms of the respiratory syncytial virus f protein. *J Virol* (2015) 89(13):6835–47. doi: 10.1128/JVI.00384-15

50. Wang J, Kong L, Luo Q, Li B, Wu J, Liu B, et al. Dual effects of respiratory syncytial virus infections on airway inflammation by regulation of Th17/Treg responses in ovalbumin-challenged mice. *Inflammation* (2014) 37(6):1984–2005. doi: 10.1007/s10753-014-9931-0

51. Connors M, Kulkarni AB, Firestone CY, Holmes KL, Morse HC3rd, Sotnikov AV, et al. Pulmonary histopathology induced by respiratory syncytial virus (Rsv) challenge of formalin-inactivated rsv-immunized Balb/C mice is abrogated by depletion of Cd4+ T cells. *J Virol* (1992) 66(12):7444–51. doi: 10.1128/JVI.66.12.7444-7451.1992

52. Delgado MF, Coviello S, Monsalvo AC, Melendi GA, Hernandez JZ, Batalle JP, et al. Lack of antibody affinity maturation due to poor toll-like receptor stimulation leads to enhanced respiratory syncytial virus disease. *Nat Med* (2009) 15(1):34–41. doi: 10.1038/nm.1894

53. Glezen WP, Paredes A, Allison JE, Taber LH, Frank AL. Risk of respiratory syncytial virus infection for infants from low-income families in relationship to age, sex, ethnic group, and maternal antibody level. *J Pediatr* (1981) 98(5):708–15. doi: 10.1016/s0022-3476(81)80829-3

54. Piedra PA, Jewell AM, Cron SG, Atmar RL, Paul Glezen W. Correlates of immunity to respiratory syncytial virus (Rsv) associated-hospitalization: Establishment of minimum protective threshold levels of serum neutralizing antibodies. *Vaccine* (2003) 21(24):3479–82. doi: 10.1016/S0264-410X(03)00355-4

55. Durant LR, Makris S, Voorburg CM, Loebbermann J, Johansson C, Openshaw PJ. Regulatory T cells prevent Th2 immune responses and pulmonary eosinophilia during respiratory syncytial virus infection in mice. *J Virol* (2013) 87 (20):10946–54. doi: 10.1128/JVI.01295-13

56. Sari D, Gupta K, Thimiri Govinda Raj DB, Aubert A, Drncová P, Garzoni F, et al. The multibac Baculovirus/Insect cell expression vector system for producing complex protein biologics. *Adv Exp Med Biol* (2016) 896:199–215. doi: 10.1007/978-3-319-27216-0_13

57. Trombetta CM, Marchi S, Montomoli E. The baculovirus expression vector system: A modern technology for the future of influenza vaccine manufacturing. *Expert Rev Vaccines* (2022) 21(9):1233–42. doi: 10.1080/14760584.2022.2085565

58. Cox MMJ. Innovations in the insect cell expression system for industrial recombinant vaccine antigen production. *Vaccines (Basel)* (2021) 9(12):1504. doi: 10.3390/vaccines9121504

59. Goodwin E, Gilman MSA, Wrapp D, Chen M, Ngwuta JO, Moin SM, et al. Infants infected with respiratory syncytial virus generate potent neutralizing antibodies that lack somatic hypermutation. *Immunity* (2018) 48(2):339–49.e5. doi: 10.1016/j.immuni.2018.01.005

60. Gorlani A, Forthal DN. Antibody-dependent enhancement and the risk of hiv infection. *Curr HIV Res* (2013) 11(5):421–6. doi: 10.2174/1570162x113116660062

61. Capella C, Chaiwatpongsakorn S, Gorrell E, Risch ZA, Ye F, Mertz SE, et al. Prefusion f, postfusion f, G antibodies, and disease severity in infants and young children with acute respiratory syncytial virus infection. *J Infect Dis* (2017) 216 (11):1398–406. doi: 10.1093/infdis/jix489

62. Ngwuta JO, Chen M, Modjarrad K, Joyce MG, Kanekiyo M, Kumar A, et al. Prefusion f-specific antibodies determine the magnitude of rsv neutralizing activity in human sera. *Sci Transl Med* (2015) 7(309):309ra162. doi: 10.1126/scitranslmed.aac4241

63. Ruckwardt Tracy J, Bonaparte Kathryn L, Nason Martha C, Graham Barney S. Regulatory T cells promote early influx of Cd8+ T cells in the lungs of respiratory syncytial virus-infected mice and diminish immunodominance disparities. *J Virol* (2009) 83(7):3019–28. doi: 10.1128/JVI.00036-09

64. Iwanaga N, Kolls JK. Updates on T helper type 17 immunity in respiratory disease. *Immunology* (2019) 156(1):3–8. doi: 10.1111/imm.13006

65. Mukherjee S, Lindell DM, Berlin AA, Morris SB, Shanley TP, Hershenson MB, et al. Il-17–induced pulmonary pathogenesis during respiratory viral infection and exacerbation of allergic disease. *Am J Pathol* (2011) 179(1):248–58. doi: 10.1016/j.ajpath.2011.03.003

66. Eichinger KM, Kosanovich JL, Gidwani SV, Zomback A, Lipp MA, Perkins TN, et al. Prefusion rsv f immunization elicits Th2-mediated lung pathology in mice when formulated with a Th2 (but not a Th1/Th2-balanced) adjuvant despite complete viral protection. *Front Immunol* (2020) 11:1673. doi: 10.3389/fimmu.2020.01673

67. Lei L, Qin H, Luo J, Tan Y, Yang J, Pan Z. Construction and immunological evaluation of hepatitis b virus core virus-like particles containing multiple antigenic peptides of respiratory syncytial virus. *Virus Res* (2021) 298:198410. doi: 10.1016/j.virusres.2021.198410

68. Schmidt MR, McGinnes LW, Kenward SA, Willems KN, Woodland RT, Morrison TG. Long-term and memory immune responses in mice against Newcastle disease virus-like particles containing respiratory syncytial virus glycoprotein ectodomains. *J Virol* (2012) 86(21):11654–62. doi: 10.1128/JVI.01510-12

69. Vicente T, Roldão A, Peixoto C, Carrondo MJ, Alves PM. Large-Scale production and purification of vlp-based vaccines. *J Invertebr Pathol* (2011) 107 Suppl:S42–8. doi: 10.1016/j.jip.2011.05.004